Journal of The Electrochemical Society, **153** (12) G1086-G1098 (2006)
0013-4651/2006/153(12)/G1086/13/$20.00 © The Electrochemical Society

Influence of the Anode and the Accelerator on Copper Bath Aging in the Damascene Process

P. Moçotéguy,[a] C. Gabrielli,[a,*] H. Perrot,[a,*] A. Zdunek,[b,*] and D. Nieto Sanz[c]

[a]*UPR 15 CNRS, LISE, Université Pierre et Marie Curie, Paris, France*
[b]*Air Liquide, Chicago Research Center, Countryside, Illinois 60525, USA*
[c]*Air Liquide, Centre de Recherche Claude Delorme, 78354 Jouy en Josas, France*

Electrochemical impedance spectroscopy and cyclic voltammetry were used to characterize the aging of copper plating baths used in damascene process for superfilling of trenches and vias in the semiconductor industry. The effects of copper anode composition, anodic current density, and accelerator nature and concentration were studied. Phosphorus added to copper anodes has a prominent impact on the evolution of current/voltage curves and impedance spectra during bath aging. The observed evolutions were explained by the formation of a Cu^I-accelerator complex in the bulk of the bath that adsorbs at the copper surface to act as an accelerating species, and by the increase of its concentration during aging with undoped copper anode. The Cu^I-accelerator complex formation is limited by the phosphorus contained in the Cu-P anode, which traps electrogenerated cuprous ions in the black anodic film. Differences observed between baths containing SPS (bis(3-sulfopropyl)disulfide) or MPSA[(3-mercaptopropane)sulfonic acid] are also attributed to the existence of two different Cu^I-accelerator complexes, both of which exhibit different formation equilibrium constants.
 [DOI: 10.1149/1.2357726]

Manuscript submitted December 15, 2005; revised manuscript received July 28, 2006. Available electronically October 20, 2006.

Dual damascene copper electroplating is commonly used for depositing the metal interconnects in integrated circuit manufacturing. Classic acid sulfate copper electroplating baths usually contain copper sulfate, sulphuric acid, and chloride ions in the range of 1 to 2 mM. However in the damascene process, acceptable superfilling of trenches and vias require the addition of several types of organic additives: brighteners/accelerators, carrier/suppressor and levelers.[1,2] Brighteners are usually propane sulfonic acid derivatives: either MPSA (HO_3S–$(CH_2)_3$–SH) or SPS (HO_3S–$(CH_2)_3$–S–S–$(CH_2)_3$–SO_3H). They accelerate the charge transfer process at the copper interface. Suppressors are often polyalkylene glycols (HO–$(C_kH_{2k}$–$O)_n$–H) that adsorb evenly at the wafer surface and increase the overpotential.

The mechanism of superfilling behavior has been explained by substitution of adsorbed suppressor compounds with accelerator additives after an induction period, and furthermore by the subsequent reduction of copper with the adsorbed accelerator.[1,3-6] Tsai et al.[7] observed that, in copper solutions containing chloride, polyethylene glycol (PEG) and MPSA, the mechanisms are identical for both the deposition and dissolution reactions. However, Dow et al.[8] recently attributed superfilling behavior to the competition between PEG and accelerator for chloride ions. These ions are complexed with the Cu^+ at the copper surface, which are widely known to be the intermediate species of both copper dissolution and deposition reaction in acidic copper sulfate baths.[9-12] In addition, among the additives used in copper electroplating baths, accelerators are found to be the least stable and most studies deal with their stability.

Healy et al.[14] observed that both MPSA and SPS oxidize at a half-wave potential of +0.68 V vs SMSE. They have also found that both these accelerators decompose at their open-circuit potential (OCP) and that a Cu^I-thiolate complex, stable in the absence of oxygen but rapidly oxidized by oxygen, acts as a key intermediate. This complex formation was associated with a color change of the solution and the replacement of the oxidation wave at +0.68 V vs SMSE by a wave at $E_{1/2} = -0.16$ V vs SMSE. Finally, they proposed the following mechanism for accelerator degradation.

1. Copper comproportionation/disproportionation reaction

$$2Cu^+ \rightleftarrows Cu^0 + Cu^{2+} \quad [1]$$

2. Generated cuprous ions react with accelerator to produce Cu^I-thiolate complex.

3. Dissolved oxygen gas reacts with the complex to produce a more oxidized product.

The Koh et al.[2] analysis of sulfur atom chemical properties toward alkyl groups and metal ions supports the complex hypothesis, as neutral sulfur ligands like R_2S have a high affinity toward transition metal ions such as copper. They also observed that the rate of the accelerator decomposition increases as suppressor concentration decreases. They explained it by the increase of Cu^+ activity with Cl^- concentration in the absence of the suppressor that will in turn increase the concentration of Cu^I-accelerator complex and thus favor its decomposition. However, when both PEG and chloride are present, they strongly bridge with the electrogenerated Cu^+ to form Cu^I-Cl-PEG complex.[14,15] Then, less Cu^+ ions are available for the formation of the Cu^I-accelerator complex, reducing the rate of accelerator decomposition.

From this standpoint, Frank and Bard[16] have shown by mass spectroscopy that, in aged baths containing $CuSO_4$, H_2SO_4, and either MPSA or SPS, the predominant species were SPS and a Cu/SPS compound. They also have shown by UV visible spectroscopy that, in fresh solutions with various MPSA concentrations, the ratio of MPS to Cu in the Cu/accelerator compound is 2:1 and confirmed that the oxidation state of copper was +1. These results suggest that a Cu^I-thiolate complex is formed, either Cu^ISPS or $Cu^I(MPSA)_2$.

Moffat et al.[17] have observed that, even without current passing, MPSA-containing solutions change within a few hours and after 24 h, exhibit the same electrochemical behavior as the fresh SPS-containing solutions, which are stable with time. To explain this behavior, they suggested the following oxidative dimerization mechanism of MPSA to SPS

$$2MPSA + 2Cu^{2+} \leftrightarrows SPS + 2H^+ + 2Cu^+ \quad [2]$$

This reaction was also confirmed by Palmans et al.[18] who observed that, as soon as Cu^{2+} was present in the plating bath, more than 99% of the MPSA was converted into SPS. In addition, such a dimerization reaction was reported by Suarez and Olson[19] for thiourea, a widely used additive in copper electrorefining processes, that dimerizes to FDS, a disulfide compound.

In addition, Moffat et al.[17] suspected that MPSA was generated during the electrolysis of SPS-containing solutions. But, Palmans et al.[18] have shown that no MPSA is formed in fresh or aged solutions of an industrial bath containing 5.6×10^{-5} M of SPS, and concluded that MPSA was unlikely formed in such bath. They finally detected two unidentified decomposition by-products in fresh solutions, whose concentrations strongly increased after the bath was aged in typical dual-damascene plating conditions. When the bath

* Electrochemical Society Active Member.

was aged beyond the typical plating conditions, five additional decomposition by-products were detected but their nature was not identified.

Concerning suppressors, Koh et al.[2] have reported that larger molecular weight polyakylene glycols could randomly cleave, either by oxidation or hydrolysis, into smaller molecules

$$HO\text{–}(CH_2\text{–}CH_2\text{–}O)_n\text{–}H + H_2O \xrightarrow{H^+} HO\text{–}(CH_2\text{–}CH_2\text{–}O)_k\text{–}H + HO\text{–}(CH_2\text{–}CH_2\text{–}O)_{(n-k)}\text{–}H \quad [3]$$

They have also reported that the suppressing effect of the polymer will be reduced substantially when its molecular weight decreases below 1000 g mol^{-1}.

Most copper interconnect plating tools use a soluble copper anode containing a small amount of phosphorus. Phosphorized copper anodes are known to behave differently than pure copper anodes in copper electroplating baths. Three different effects have been reported.[13,20,21]

1. Phosphorus, even in tiny amounts, abruptly decreases the electrical conductivity of copper. Because phosphorus, like many other impurities, preferentially concentrates along intergranular boundaries, the phosphorus hinders their dissolution, favoring homogeneous grain dissolution and preventing slime formed by the detachment of complete crystal grains from the crystalline structure.[13] This slime is detrimental for copper deposit quality.

2. The black anodic film produced during the dissolution of phosphorus containing copper anodes enhances anodic dissolution, which proceeds with lower overvoltage.

3. Phosphorus promotes direct oxidation of copper metal to Cu^{2+}, counteracting the chloride ion effect and preventing the slime formation associated with the poor adhesion of the CuCl film formed at electrode surface.[8,20,22-25]

In a previous work,[26] we made impedance measurements in fresh solutions with various concentrations of MPSA or SPS. Unexpectedly, Reaction 2 appeared to be insignificant since the impedance spectra obtained in solutions containing a given concentration of MPSA were different than those obtained for half of this given concentration of SPS. In another study,[27] we also observed that the evolution during aging of a bath containing 10^{-5} M of MPSA was different, depending on the anode material used (pure copper or phosphorized copper anode). This bath was more stable when aged with a phosphorized copper anode.

As far as we know, besides these previous works,[26,27] extensive studies have not been undertaken during long plating bath aging to understand the interactions between copper anode materials, accelerator nature, and concentration on copper plating bath evolution. To gain additional insight into these phenomena, the effect of various operating conditions on baths aging behavior was studied with respect to the anode material, the aging anodic current density, and the nature and the concentration of the accelerator.

Experimental

All the studies were performed with a bath containing 1.8 M H_2SO_4 + 0.25 M $CuSO_4$ + 10^{-3} M NaCl + 88 × 10^{-6} M PEG as base solution to which different concentrations of accelerator (either SPS or MPSA) were added. The PEG used in this study had a 3400 g mol^{-1} molecular weight. For reference, an MPSA concentration of 10^{-5} M in this type of bath is known to provide superfilling in submicrometer cavities.[1,3] All experiments were performed at 25°C.

The influence of the following parameters on bath aging was studied.

Anode material.— Two different anode materials were evaluated: a phosphorized copper anode from Metal Samples, Inc., containing 0.024 wt % of phosphorus and a Goodfellow 99.99%+ copper anode (called "undoped" or "pure" copper anode in this paper).

Table I. Operating conditions used to study the influence of anodic current density on copper plating bath aging.

Experiment N^r	1	2	3
Set current (A)	1.21	1.22	0.12
Anode surface area (cm^2)	24.4	48.75	120
Anodic current density (mA cm^{-2})	50	25	1
Cathode surface area (cm^2)	48.75	48.75	4.8
Cathodic current density (mA cm^{-2})	25	25	25
Experiment duration (h)	>8	>8	>80
Total charge amount (Ah L^{-1})	>14	>13.7	>13.8

The other experimental conditions are identical to experiment 2 in Table I. Because it was previously observed[27] that an inert anode material was detrimental to copper bath evolution during aging, the study with such materials was not pursued.

Anodic aging current density.— The operating conditions are reported in Table I.

Accelerator nature (SPS or MPSA) and concentration.— MPSA concentration was varied from 0 to 10^{-4} M. Because MPSA is expected to be converted to SPS according to Reaction 2, the SPS concentration was fixed at 5 μM, to keep the bath's superfilling properties constant. Other experimental conditions are identical to experiment 2 in Table I.

The experimental set up, with a solution volume of 0.7 L, contained two independent electric circuits: an aging circuit where copper deposition was carried out, and an independent characterization circuit where the voltammetric and EIS measurements were conducted.

The aging circuit consisted of a saturated mercurous sulfate reference electrode (SMSE), an anode (phosphorized copper or pure copper), and a 99.9% industrial grade copper cathode, acting as the deposition substrate. During bath aging, both the anode and cathode potentials were monitored with time and the plating bath was stirred with a magnetic stirrer. Both anode and cathode active areas were controlled using a TFM Electromask green insulating resin, supplied by Henkel. The electrochemical characterization circuit contained an additional saturated mercurous sulfate electrode, an anode sheet whose material was identical to the one used in the anode aging circuit, and a rotating disk working electrode (0.2 cm^2 active area) rotated at 2000 rpm during the experiments. The disk electrode consisted of a 5 mm diam Goodfellow 99.99%+ copper rod embedded in an inert and insulating Presi allylic glass fiber resin. It was polished with a 1200 grade SiC paper and rinsed with deionized water to clean the surface before measurement.

Solutions were prepared the day before and stored overnight in sealed volumetric flasks without any electrode. Electrodes were inserted in the solution just before current setting. Bath aging was characterized in two different ways: cyclic voltammetry (CV) and impedance spectroscopy. The CVs were obtained using an Autolab PGSTAT100 potentiostat/galvanostat. The potential was swept cathodically from the OCP down to −0.75 V vs SMSE (or −0.8 V when solutions without accelerator were studied) and then back to the initial OCP at a 0.5 mV s^{-1} scan rate. The impedance spectra were measured using a Solartron 1250 frequency response analyzer. Data acquisition was performed at different times during aging using a software program designed by the CNRS/LISE laboratory. The spectra were acquired in a frequency range of 62.5 kHz down to 10 mHz, in galvanostatic mode at a 25 mA cm^{-2} average deposition current density.

Because bath aging still occurs during the bath characterization steps, the aging charge amount range corresponding to each measurement was reported in the graphs. The aging charge amount is defined as the amount of charge passed in the aging circuit per unit volume (Ah L^{-1})

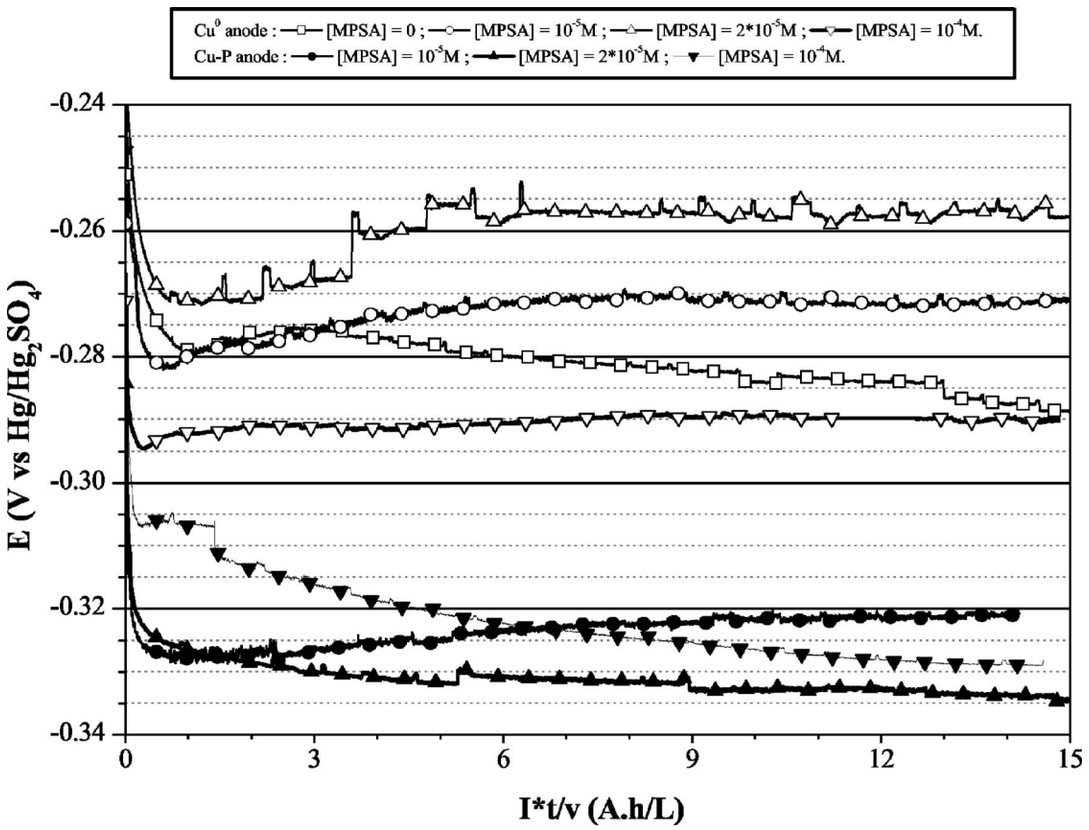

Figure 1. Influence of anode material and MPSA concentration on copper dissolution potential evolution during aging with a 25 mA cm^{-2} current density.

Results

Figure 1 shows that, for a concentration of MPSA between 10^{-5} and 10^{-4} M, the addition of a small amount of phosphorus in the anode induces a significant decrease of between 30 and 70 mV in the copper dissolution potential as compared with the undoped copper anode. This suggests that the copper dissolution kinetics increases with the doping of phosphorus into the pure copper anode. This result is consistent with those published in the literature.[13,20,21] Such acceleration of copper dissolution kinetics by phosphorus was also observed in the SPS-containing bath.

Figure 2 clearly shows that the presence of phosphorus in a copper anode can strongly impact the copper deposition kinetics by slowing the copper deposition at the cathode during the whole aging process. When the bath was aged with an undoped copper anode, whatever the accelerator nature, the copper deposition potential almost continuously increases with aging. In addition, a cusp in the I-V curve was observed in the plot for MPSA-containing baths, indicating that a specific reaction occurs at the beginning of aging. Dow et al.[8] also observed such a cusp in the curve after injection of 4 ppm MPSA to a solution containing 0.54 M H_2SO_4 + 0.88 M $CuSO_4$ + 60 ppm chloride and attributed it to the transient formation and consumption of CuCl precipitates. When a 10 μM MPSA-containing bath was aged with a phosphorized copper anode, a strong increase of the deposition potential was observed up to a maximum followed by a decrease down to an almost steady state value.

Figure 2 also shows that the nature of the accelerator strongly impacts the copper deposition kinetics. Indeed, the "cusp" observed for MPSA containing bath aged with pure copper anode did not appear so clearly in the SPS containing solutions, even if an inflection is observed in the potential evolution. These results are consistent with those of Dow et al.[8] who did not observe a cusp in the curve after the injection of 4 ppm SPS. Moreover, if the copper deposition potential evolutions during aging with a pure copper anode are parallel for SPS- and MPSA-containing baths, the copper deposition kinetics are much slower (about 40 to 60 mV lower) in the former. When the bath was aged with a phosphorized copper anode, the potential evolution at the beginning of aging was also influenced by the nature of the accelerator: a continuous increase in the potential was obtained for the SPS containing bath while a transient maximum was observed in the MPSA containing bath. However, after a few $A.h.L^{-1}$ of aging, both potential evolutions were close. It thus appears that Reaction 2 is at least incomplete.

Figure 3 indicates that the effect of the anode material is much more important for high anodic current densities This difference between high and low anodic current densities can not be attributed to an ohmic drop effect due to the differences in the applied current intensity, as the curves (not shown here) represented with respect to time do not exhibit parallel evolutions.

Electrochemical characterization of plating bath aging.— Figure 4a and b present, for each type of anode material, the evolution with aging of the voltammograms recorded in a bath containing 10^{-5} M of MPSA and aged at 25 mA cm^{-2}. The CVs exhibit a large hysteresis, with the forward scan occurring at more negative potentials than the backward scans. This hysteresis has been previously ascribed to the substitution of PEG molecules adsorbed at copper surface by MPSA molecules.[1,4,5] The hysteresis amplitude was reduced by the use of a phosphorized anode, mainly because the backward scan proceeds at lower current densities.

In addition, a high stability in the copper deposition kinetics was observed when the bath was aged with a phosphorized copper anode. The changes in the current/voltage curves are negligible when a charge amount greater than 2 Ah L^{-1} was passed. This is in accor-

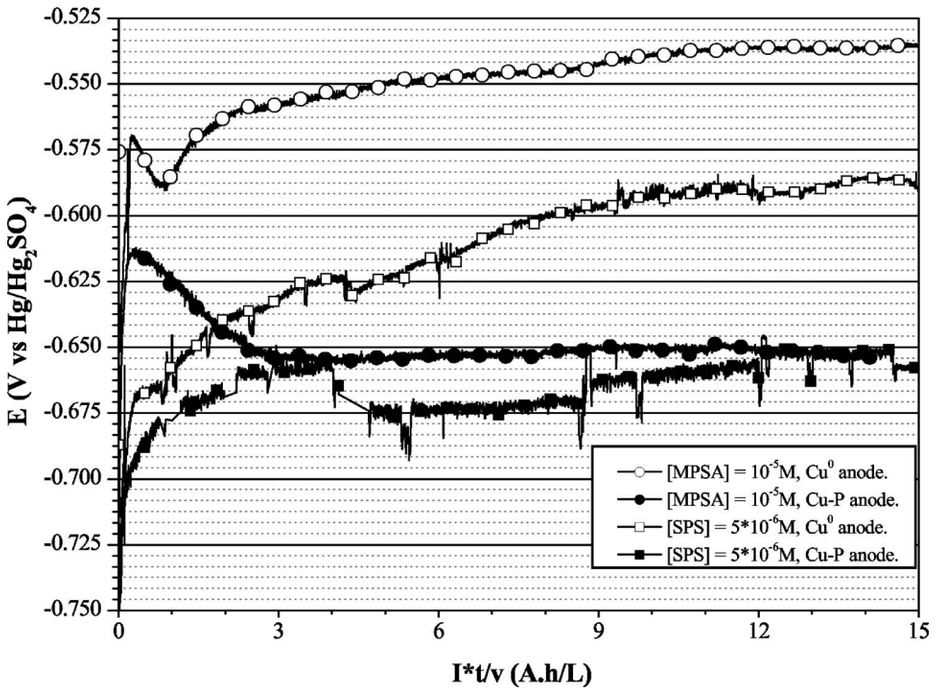

Figure 2. Influence of accelerator nature and anode material on the evolution of copper deposition potential during bath aging with a 25 mA cm^{-2} current density.

dance with the copper deposition potential evolution of the aging circuit (Fig. 2). On the other hand, when the bath is aged with a pure copper anode, a slight and transient shift at the very beginning of aging to a more negative potential is observed that correlates with the small cusp in the I-V curve observed in Fig. 2 for the copper deposition evolution with time. Then, the current/voltage curves are continuously translated to less negative potentials as bath aging proceeds. This means that the copper deposition kinetics is accelerated. Moreover, when a phosphorized copper anode was used, at the very beginning of aging, a distinct reduction wave appears in the voltammogram for low deposition current densities, pointing out an effect of phosphorus in the soluble anode on the deposition reactions. (see inset of Fig. 4b).

These evolutions are also valid in SPS-containing solutions: the copper deposition kinetics are enhanced when the bath is aged with a pure copper anode while the current/voltage curves stabilize after the passage of 1.5 Ah L^{-1} charge amount when a phosphorized copper anode is used.

However, close observation of Fig. 5a shows that, at the very

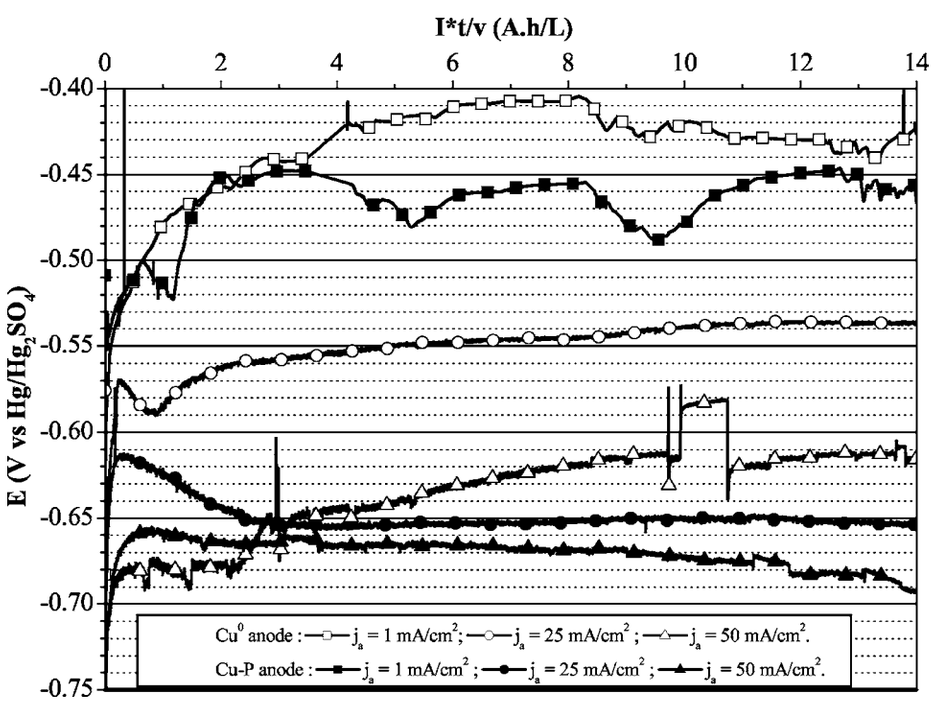

Figure 3. Influence of anode material and aging anodic current density on the evolution of copper deposition potential during aging with a 25 mA cm^{-2} current density.

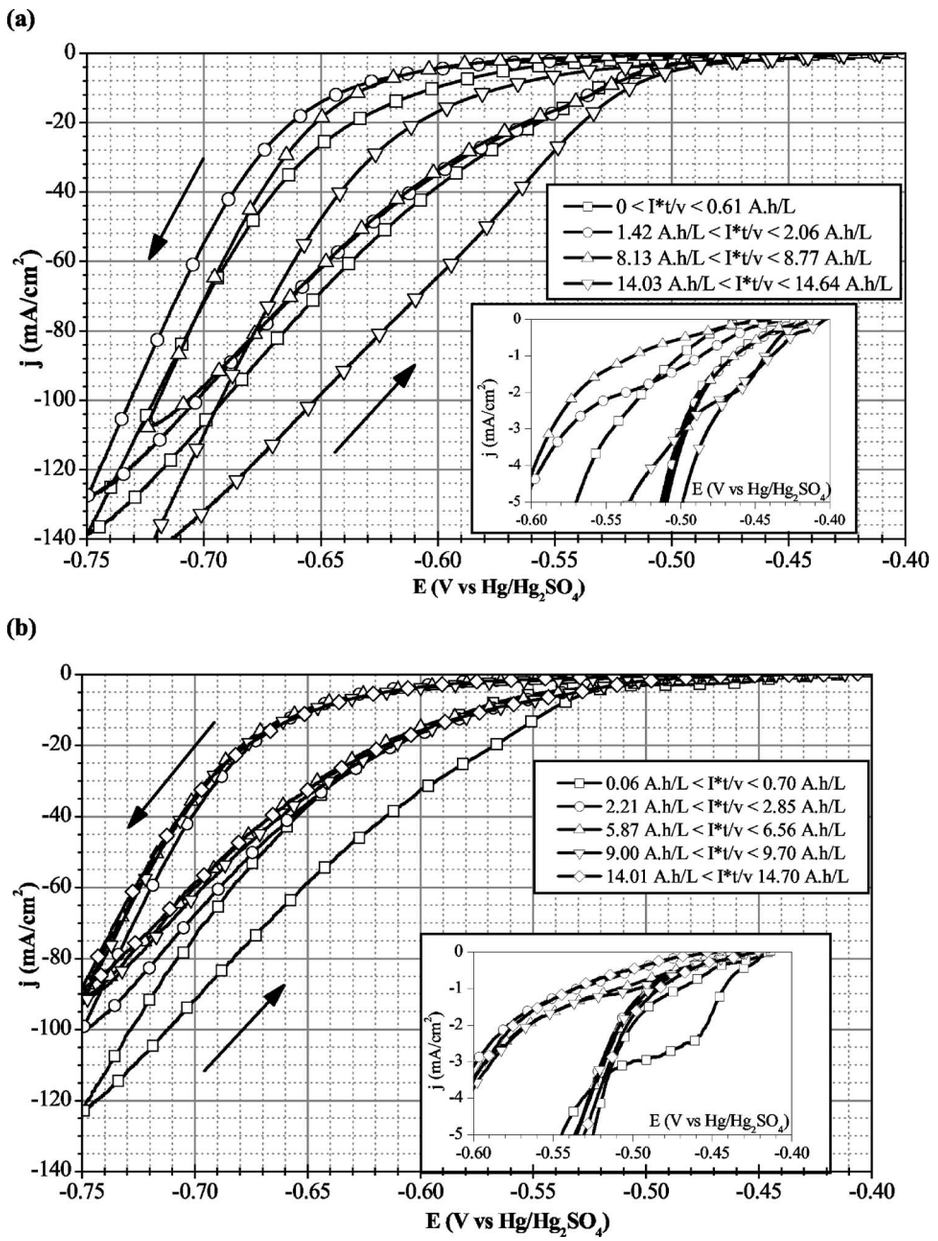

Figure 4. Influence of anode material on the evolution of current-voltage curves with aging of a bath containing 10 μM MPSA and aged with a 25 mA cm^{-2} current density. (a) Goodfellow 99.99%+ copper anode. (b) Copper anode containing 0.024 %w/w+ of P. (Voltage scan rate 0.5 mV s^{-1}.)

beginning of aging, there is significant differences between the behavior of SPS- and MPSA-containing baths, indicating that Reaction 2 is at least incomplete.

1. The first reduction wave obtained in MPSA containing solution aged with phosphorized copper anode did not appear in the SPS containing bath (see inset).

2. The hysteresis obtained when bath is aged with a phosphorized copper anode is much more important in SPS-containing bath than in a MPSA-containing bath.

3. The hysteresis obtained in MPSA-containing bath is much less important when bath is aged with a phosphorized copper anode than when it is aged with a pure copper anode, while this effect is not observed for SPS-containing baths.

4. The substitution of the PEG by the accelerator is faster in MPSA-containing baths than in SPS-containing baths because, whatever the anode material, the forward scan occurs at less negative potentials. This result is in accordance with those of Fig. 2.

As bath aging proceeds, the effect of the nature of the accelerator tapers off while the effect of aging anode material becomes prominent (cf. Fig. 5b and c). This result is in accordance with those of Fig. 2.

When the MPSA concentration was increased from 10 to 20 μM, the evolution of the current/voltage curves observed for both anode materials are similar as seen in Fig. 4 and in Fig. 6a and b. However, some differences appear, including:

1. Copper deposition kinetics are accelerated by the increase in MPSA concentration, when the bath was aged with a pure copper anode (Fig. 6a),

2. The hysteresis behavior progressively tends to disappear as bath aging proceeds, indicating that the mechanism of MPSA substitution for PEG is not present. This was not the case when a phosphorized copper anode was used: the amplitude of the hysteresis increased even when bath aging proceeded (Fig. 6b), and

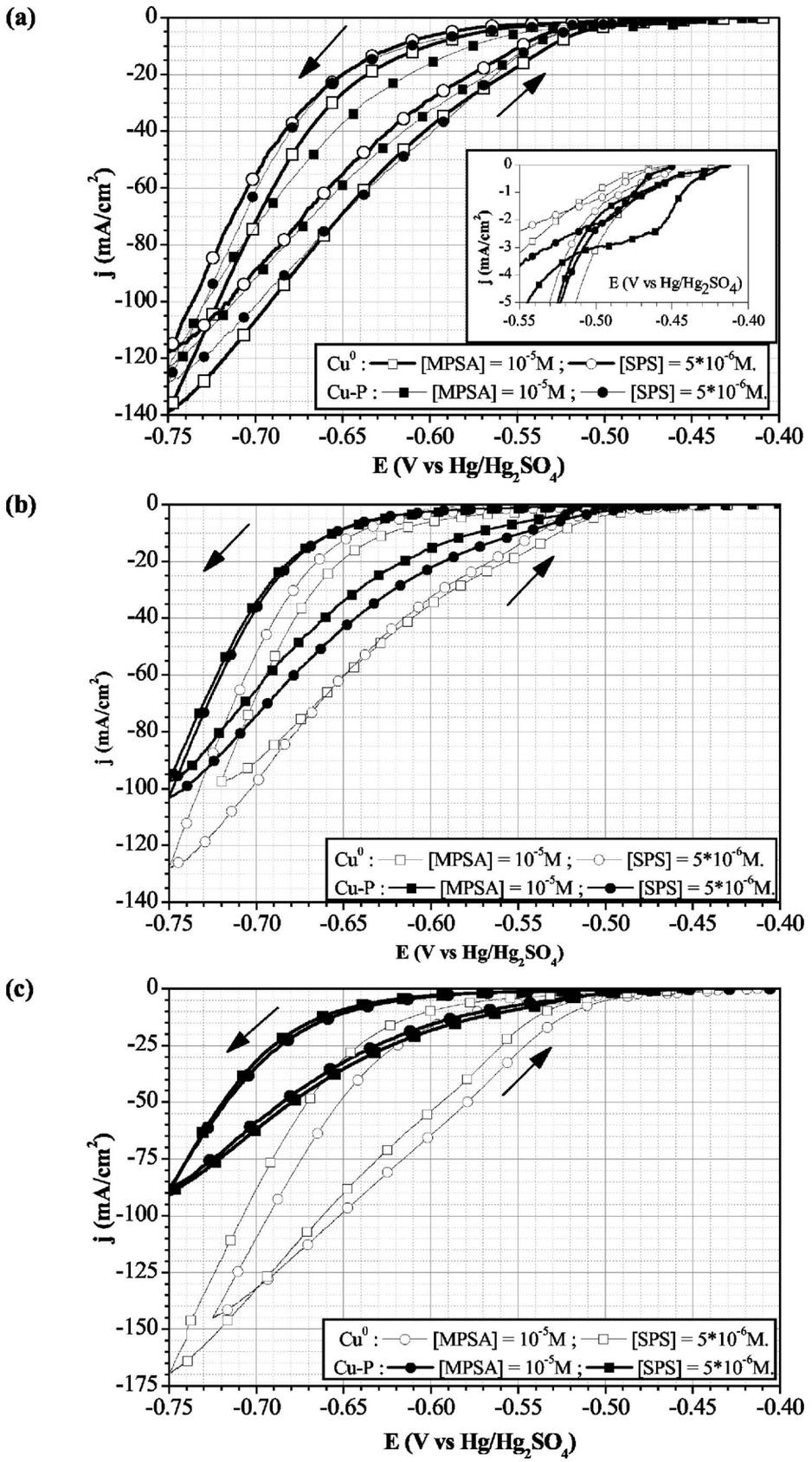

Figure 5. Influence of aging anode material and accelerator nature on the current-voltage curves recorded for different aging charge amounts (Voltage scan rate 0.5 mV s^{-1}, aging current density 25 mA cm^{-2}). (a) $0 < I^*t/v < 0.7$ Ah L^{-1}, (b) 4 Ah $L^{-1} < I^*t/v < 4.9$ Ah L^{-1}, (c) 13.9 Ah $L^{-1} < I^*t/v < 14.7$ Ah L^{-1}.

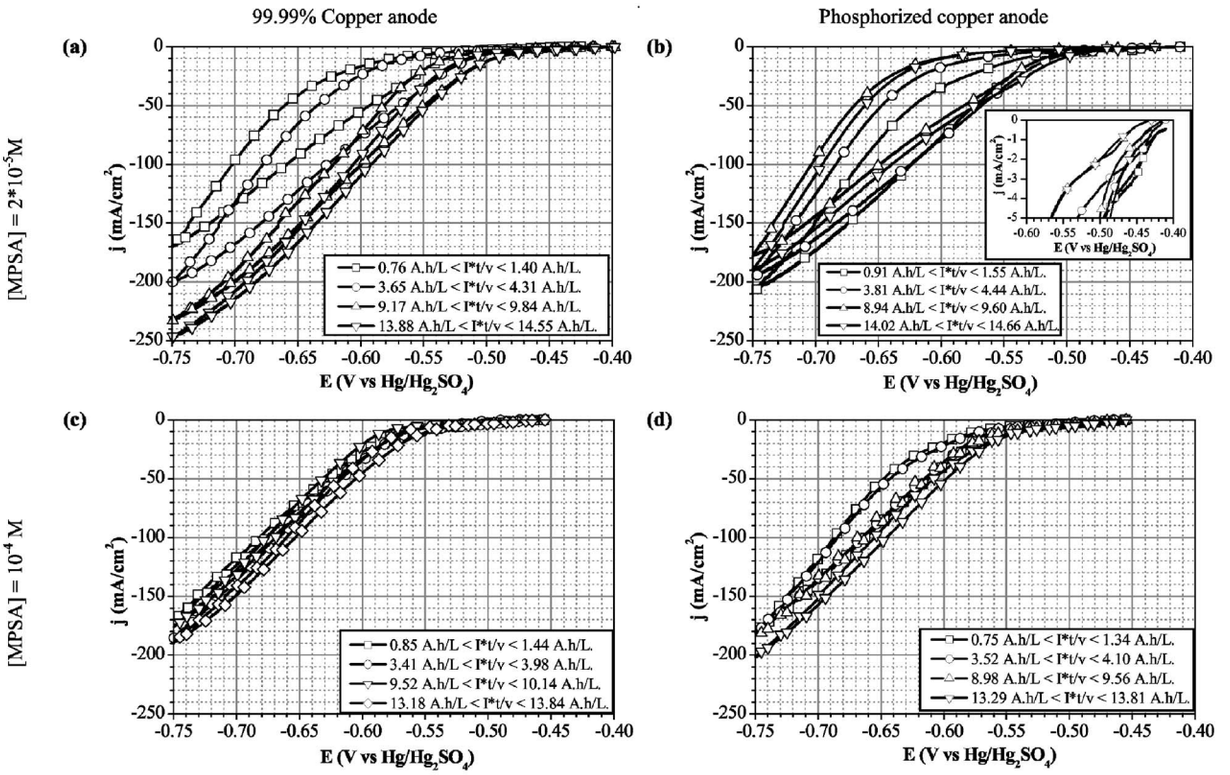

Figure 6. Influence of anode material and MPSA concentration on the evolution of current-voltage curves with aging. Aging anodic current density 25 mA cm^{-2}. Anode material are (a) and (c) Goodfellow 99.99%+ copper anode, (b) and (d) copper anode containing 0.024 %w/w of P. MPSA concentrations are (a) and (b) 20 μM MPSA, (c) and (d) 100 μM. (Voltage scan rate 0.5 mV s^{-1}.)

3. The distinct reduction wave appearing at the very beginning of aging with a phosphorized copper anode was almost eliminated (inset of Fig. 6a).

When MPSA concentration is further increased in the bath to 100 μM (Fig. 6c and d), once again, the anode material effect is prominent. When the bath was aged with a pure copper anode (Fig. 6c), we noticed that copper deposition is less accelerated than in baths containing 20 μM MPSA. Therefore, the accelerating effect of MPSA on copper deposition kinetics was lowered if its concentration increased too much. These results are consistent with those of Suarez and Olson[19] who observed the same phenomenon for thiourea. Moreover, very little hysteresis appears on the CVs, despite the presence of both PEG and MPSA and the CVs exhibit little evolution with time. Conversely, when the bath is aged with a phosphorized copper anode (Fig. 6d), the hysteresis behavior is present at the beginning of the aging process but almost disappears after 4.9 Ah/L of charge has passed. This behavior is identical to the one observed in a bath containing 20 μM of MPSA aged with a pure copper anode (Fig. 6a). Moreover, it can also be noted from comparison between Fig. 6b and d that the forward scan proceeds with lower overvoltage in a bath containing 100 μM of MPSA than in a bath containing 20 μM of MPSA, while the backward scan proceeds roughly with the same overvoltage.

Finally, in a bath without MPSA, no hysteresis is observed in the current/voltage curves and the deposition reaction is accelerated by the aging process (Fig. 7). This can be explained by the PEG cleaving Reaction 3 and the need for a sufficiently high molecular weight to insure that the PEG inhibition effect[2] is taken into account.

Figure 8 presents the evolution of the current/voltage curves recorded when the bath was aged at a 1 mA/cm^2 current density with a phosphorized copper anode. At the very beginning of aging, a distinct reduction wave is observed which is very similar to the wave obtained when the bath was aged at a 25 mA cm^{-2} anodic current density (see inset). After about 5 Ah L^{-1} of charge (corresponding to about 28 h of aging), the hysteresis phenomenon disappeared. Furthermore, a continuous shift of the voltage curves toward less negative deposition potentials was observed. This behavior was also seen when the bath was aged with a pure copper anode and is very similar with the one previously obtained when the bath was aged at 25 mA cm^{-2} with a glassy carbon anode.[27] For glassy carbon anode, it was proposed that rapid accelerator decomposition due to both very high anodic potentials (~2 V vs SMSE) and strong oxygen evolution, followed by a PEG molecules cleaving according to Reaction 3, could explain these features. However, in this experiment, the anodic potential remained low (between −0.37 and −0.35 V vs SMSE) and no oxygen evolution was observed.

When the bath was aged with a pure copper anode, a similar current/voltage curve evolution was observed, except for the distinct reduction wave at very low current density that was not observed (not shown here). The evolutions were slightly faster when bath was aged with pure copper anode.

Electrochemical impedance measurements.— Figure 9 compares the evolutions of the impedance spectra recorded during bath aging with a 25 mA cm^{-2} anodic current density as a function of both anode material and accelerator. When the MPSA-containing bath was aged with a pure copper anode, the impedance spectra exhibits an inductive loop that slowly grows in the initial stages of aging and then stabilizes (Fig. 9a). The formation of a small third capacitive loop was also observed. On the other hand, when this bath is aged with phosphorized copper anode, the small inductive loop appearing at low aging charge amount rapidly vanishes and no third capacitive loop appears (Fig. 9b).

Comparison of Fig. 9b and d shows that the impedance spectra

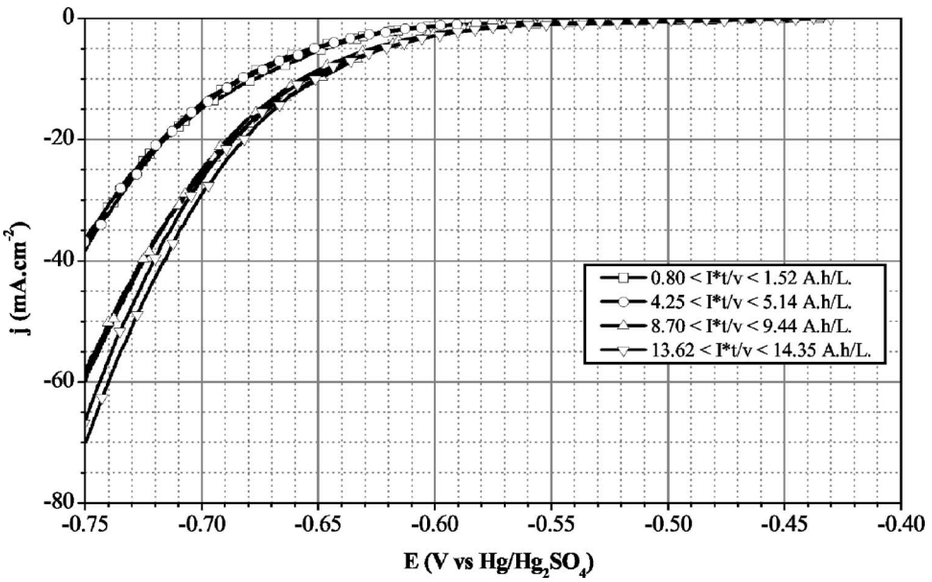

Figure 7. Evolution of current-voltage curves with aging for a bath containing no MPSA and aged with a Goodfellow 99.99%+ copper anode operating at 25 mA cm^{-2}. (Voltage scan rate 0.5 mV s^{-1}.)

obtained during aging with a phosphorized copper are similar for both accelerators. The only difference is that the small inductive loop obtained at the very beginning of aging does not appear in the SPS-containing bath. However, when a pure copper anode is used, as shown by Fig. 9a and c, the evolution of the inductive loop during bath aging is very different for the two accelerators. With the SPS additive, a roughly continuous increase of the size of the inductive loop is observed. With the MPSA additive, the size of the inductive loop first increases at the beginning of aging (until about 5 $A.h.L^{-1}$ of charge had passed), stabilizes and finally decreases for high aging charge amount. With both accelerators, the inductive loop is associated with a small third capacitive loop. The results could be interpreted by faster bath degradation for MPSA-containing baths than for SPS-containing baths.

It thus appears that:

1. The anode material effect is more important than the accelerator nature effect. A pure copper anode is needed to observe an effect of the nature of the accelerator. Indeed, with a phosphorized copper anode, there is practically no difference for the accelerator.

2. Because the impedance spectra exhibit different evolutions, the composition of MPSA- and SPS-containing bath is different, which means that Reaction 2 is at least incomplete, and might even be not significant in our experimental conditions.

To better understand these evolutions, a parameter linked with the size of the inductive loop was calculated from each impedance spectrum, according to

$$D_{IL} = \text{Max}(\text{Re}(Z)) - \text{Re}(Z_{10\ mHz}) \quad [4]$$

Figure 10 presents the influence of anode material and the nature of the accelerator on the evolution of the size of the inductive loop with bath aging, as calculated by Eq. 4. This graph highlights the high effect of phosphorus contained in the anode on the evolution of the bath during aging and the differences between SPS- and MPSA-containing baths. In addition, it shows that the increase of D_{IL} with aging is slower in SPS-containing baths than in MPSA-containing baths, indicating that latter bath changes faster with aging.

Figure 11 presents the influence of the anode material and the

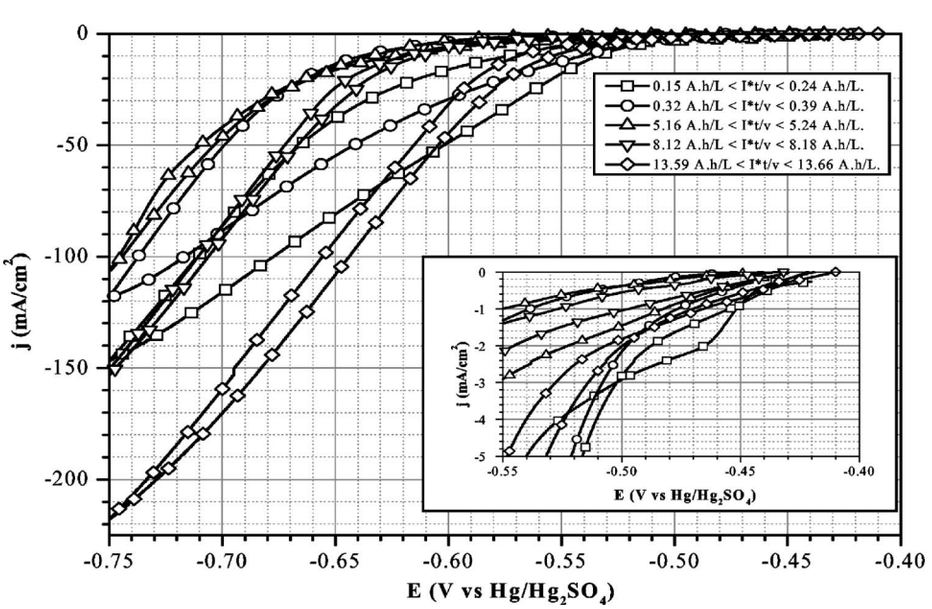

Figure 8. Evolution of current-voltage curves with aging for a bath containing 10 μM MPSA and aged with a copper anode containing 0.024 vol % of P and operating at 1 mA cm^{-2}. (Voltage scan rate 0.5 mV s^{-1}.)

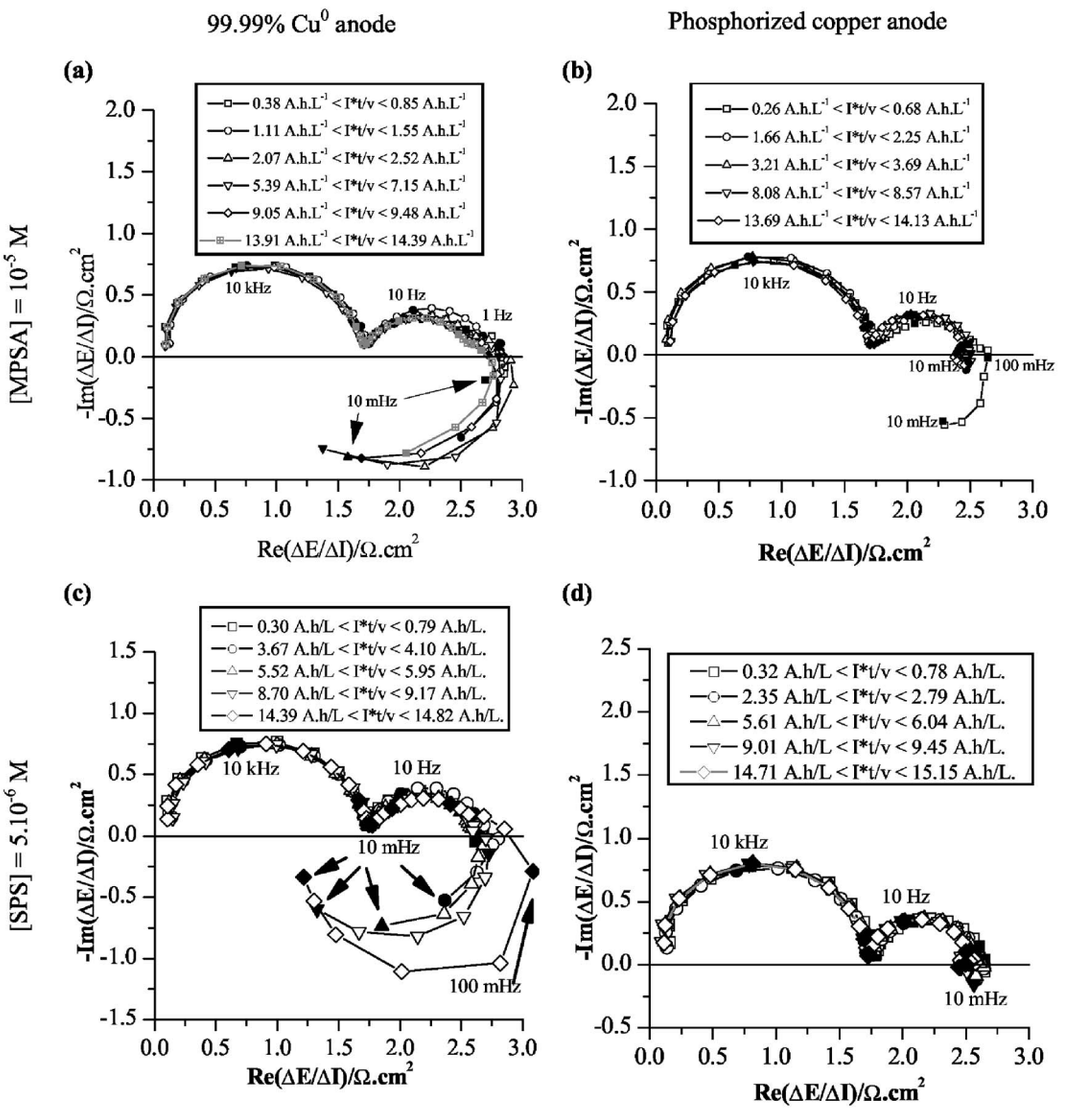

Figure 9. Influence of accelerator nature and anode material on the evolution of the impedance spectra during aging with a 25 mA cm^{-2} current density.

MPSA concentration on the evolution of the size of the inductive loop with bath aging, as calculated by Eq. 4. For the lowest values of the MPSA concentration (10 and 20 μM), once again, the strong effect of the anode material was noticed. For a phosphorized copper anode, the size of the inductive loop decreases as aging proceeds, while it increases when a pure copper anode is used. The decrease is faster when the initial MPSA concentration in the plating bath is lower. For high MPSA concentrations (100 μM), a large inductive loop was observed in the impedance spectra for whatever anode material used. The size of the loop changes during bath aging, and roughly follows a flattened bell shape.

Figure 12 shows that the impedance spectrum of a solution containing no accelerator and aged with a pure copper anode is not affected at all by the aging process. Moreover, even if a tiny inductive loop is observed, its size is much lower than the one observed during the aging of accelerator containing baths. This graph thus clearly shows that the large inductive loops observed when accelerator molecules are present are really associated with the accelerator and not with the suppressor.

Figure 13 shows the effect of anode material on bath evolution is still paramount when the aging anodic current density is increased from 25 to 50 mA cm^{-2} However, several differences appear:

1. For the phosphorized anode, the initial inductive loop obtained at 25 mA cm^{-2} did not occur and a reduction in the size of the second capacitive loop, that was previously associated with chloride ion adsorption as CuCl,[28] was observed.

2. For the pure copper anode, the increase in the aging anodic current density slowed the evolution of D_{IL}. Indeed, the rate of increase of the D_{IL} value was halved when the aging anodic current density was doubled. However, at this stage, it is necessary to point out that a very high amount of copper particles were released in the bath during this experiment, which is known to be detrimental to the quality of the copper deposits.[13,20,21]

When the bath was aged using a 1 mA cm^{-2} anodic current density, it aged faster than when it was aged at higher anodic current densities. For example, when the bath is aged with a pure copper anode with a 1 mA cm^{-2} anodic current density, the maximum of the D_{IL} value is reached as soon as 0.9 Ah L^{-1} of charge had passed while 4 Ah L^{-1} was needed when bath was aged with a

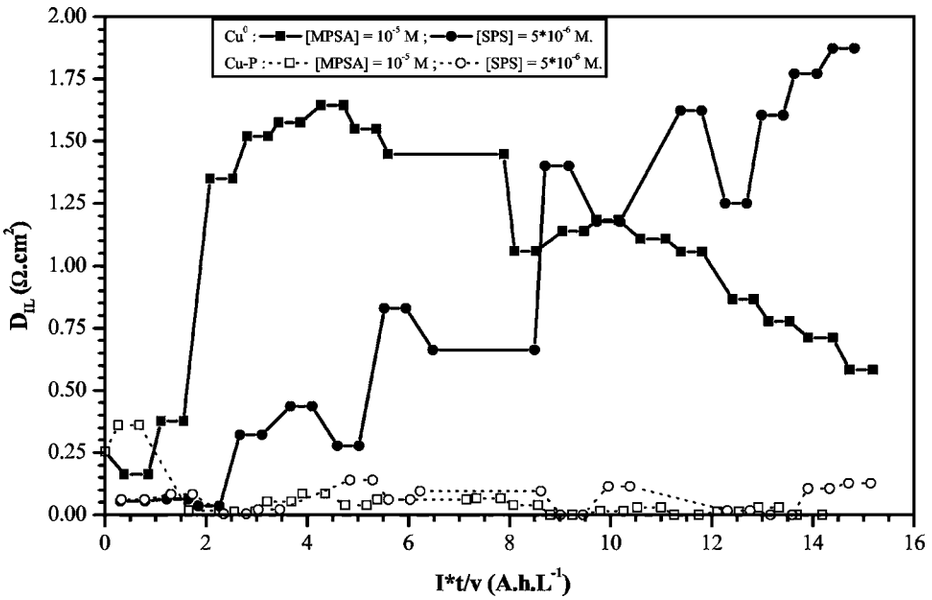

Figure 10. Influence of anode material and accelerator nature on the evolution of the size of the inductive loop during bath aging with a 25 mA cm^{-2} current density.

25 mA cm^{-2} anodic current density (Fig. 13). Moreover, even in the bath aged with the phosphorized copper anode, both the inductive loop and the third capacitive loop are observed (Fig. 14). Therefore, the previously observed effect of the phosphorus seems to vanish. In addition, for high aging charge amount ($I^*t/v > 12$ Ah L^{-1} for bath aged with pure copper anode and $I^*t/v > 8$ Ah L^{-1} for bath aged with phosphorized copper anode), the impedance spectra dramatically changed: the second capacitive loop, that was previously associated with chloride ions adsorption at copper surface[28] was strongly reduced (Fig. 14).

Discussion

Because all the compounds needed for its existence are simultaneously present in the plating bath, the Cu^I-accelerator complex identified in the literature[2,8,14,16-18,27] most likely has formed in the bulk bath and is in equilibrium with its constituents, according to

$$Cu^+ + n\text{Acc} \rightleftarrows Cu^I(\text{Acc})_n \quad [5]$$

The equilibrium concentration of free Cu^+ can be determined on the basis of the thermodynamic equilibrium constant of Reaction 1

$$K_1 = \frac{[Cu^+]^2}{[Cu^{2+}]} = 5.6 \times 10^{-7} \text{ M} \quad [6]$$

as reported in Ref. 2.

Thus, in our experimental conditions where $[Cu^{2+}] = 0.25$ M, the concentration of free Cu^+ can be calculated at 3.74×10^{-4} M, a value higher than the accelerator concentrations used in this study. On the basis of the results of Frank and Bard,[16] in Eq. 5, $n = 1$ if accelerator is SPS and $n = 2$ if accelerator is MPSA. Moreover, according to the thermodynamics of equilibrium, the complex formation's equilibrium constant is defined by

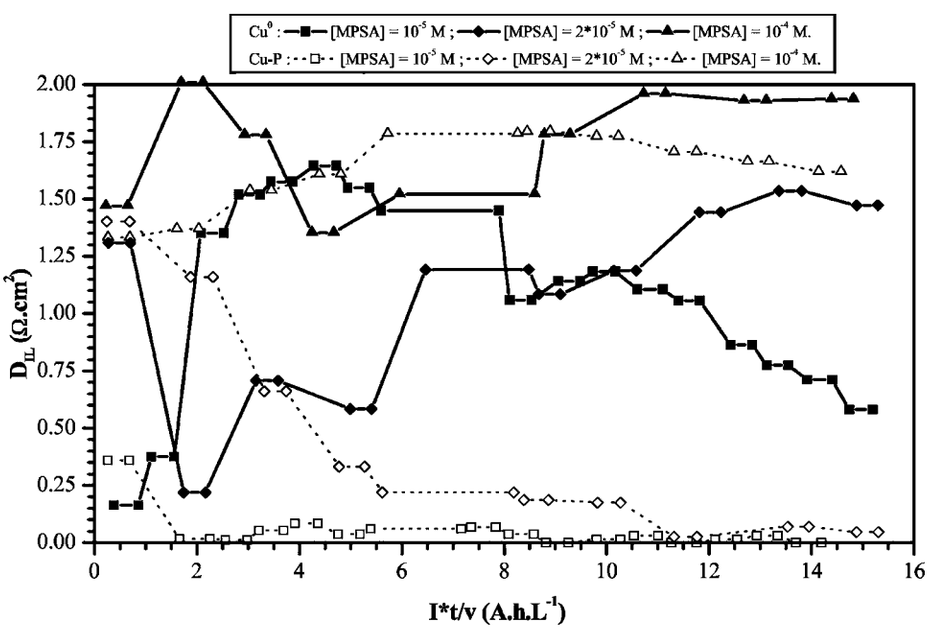

Figure 11. Influence of anode material and accelerator concentration on the evolution of the size of the inductive loop during bath aging with a 25 mA cm^{-2} current density.

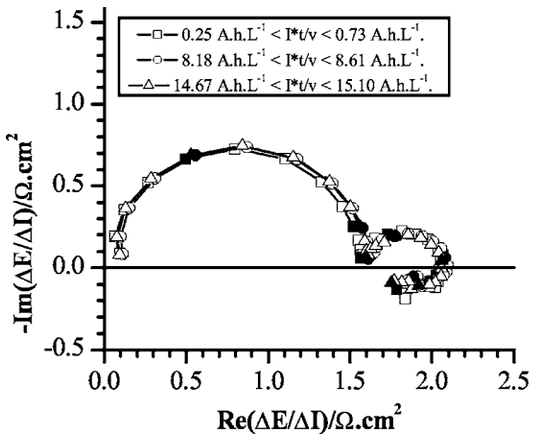

Figure 12. Evolution of the impedance spectra with aging for a bath containing no MPSA and aged with a Goodfellow 99.99%+ copper anode operating at 25 mA cm^{-2}.

$$K_{f,Cu^{I}(Acc)_n} = \frac{[Cu^{I}(Acc)_n]}{[Cu^{+}][Acc]^{n}} \Leftrightarrow [Cu^{I}(Acc)_n] = K_{f,Cu^{I}(Acc)_n}.[Cu^{+}].[Acc]^{n} \quad [7]$$

Such complex formation can occur in the bulk and implies a ligand bonding between a lone pair of electrons of a sulfur atom and the 3d orbital of a copper ion, without electron transfer such as in an oxydo-reduction reaction.[2,8]

According to Eq. 7, the amount of Cu^{I} accelerator complex in the bath is directly correlated with the bulk concentrations of both the accelerator and the free Cu^{+}. An increase in either Cu^{+} or MPSA concentrations in the bulk stabilizes the complex. In addition, it is well known[13,20,21] that phosphorized copper inhibits the Cu^{+} release in the plating bath by favoring direct oxidation of Cu^{0} to Cu^{2+} or by trapping the anodically generated Cu^{I} species in the stable black anodic film while a pure copper anode is known to release high amounts of Cu^{+} ions in the bath.

In previous studies,[26,29] we simulated the impedance spectra obtained from the same copper plating baths used in this study and modeled the copper deposition mechanism using the competitive adsorptions of a Cu^{I}-Cl-PEG complex and the Cu^{I}-accelerator com-

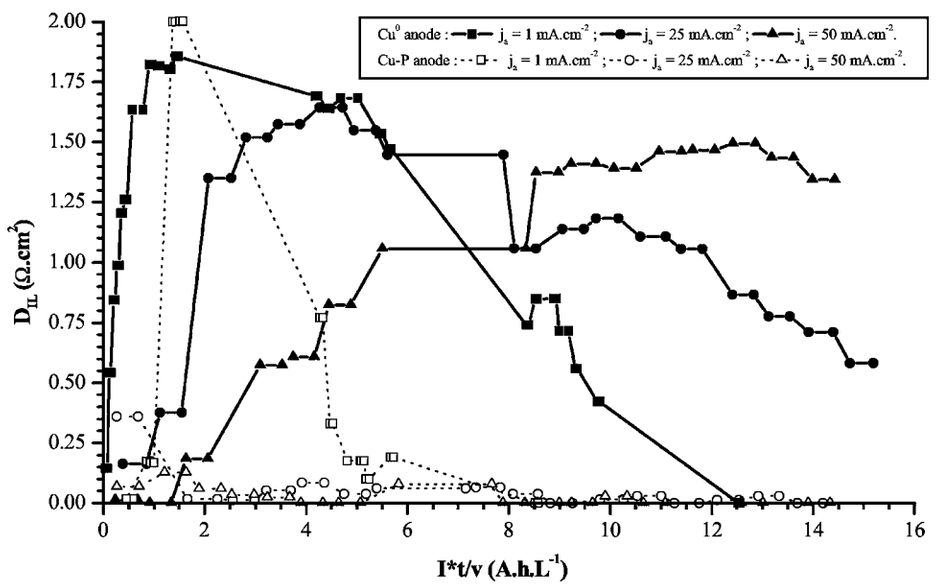

Figure 13. Influence of anode material and aging anodic current density on the evolution with bath aging of the size of the inductive loop obtained by impedance with a 25 mA cm^{-2} current density.

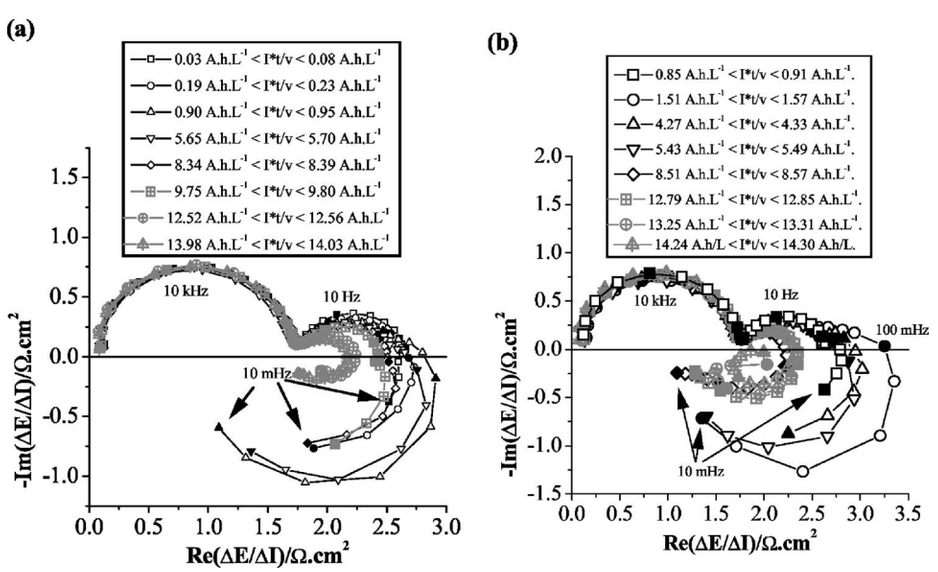

Figure 14. Influence of anode material on the evolution of the impedance spectra during aging with a 1 mA cm^{-2} anodic current density; (a) pure copper anode, (b) phosphorized copper anode.

plex. Our simulations were able to correctly fit our experimental results and have shown that the formation and the size of the inductive loop, as defined in Eq. 4, were directly correlated with the Cu^I-accelerator surface coverage. We also have shown that, the Cu^I-accelerator complex surface coverage increases with its concentration in the plating bath. In addition, Fig. 12 clearly shows that the large inductive loops can only be associated with accelerator molecules.

As a consequence, in this study, the progressive increase in the size of the inductive loop during bath aging with a pure copper anode can be interpreted by an increase in the amount of Cu^I-accelerator complex during bath aging. This increase can in turn be explained by the accumulation of Cu^+ ions released in the bath by anodic dissolution. Indeed, as reported by Frankel et al.,[20] the disproportionation Reaction 1 is slow in homogeneous media and needs a catalytic surface, such as copper metal to proceed at significant rate. Thus, if the rate of Cu^+ release due to anodic dissolution is higher than its disproportionation rate, the amount of Cu^+ in the bath increases, which stabilizes the Cu^I-accelerator complex. This, in turn, explains the progressive disappearance of the inductive loop when the aging current is switched off.[27,29] The progressive decrease in the size of the inductive loop after long aging times can in turn be explained by a decrease in the complex concentration due either to its own degradation or to the accelerator degradation as aging proceeds.

Conversely, the phosphorus contained in a phosphorized copper anode inhibits the Cu^+ release which does not accumulate in the plating bath. This, is turn, limits the amount of Cu^I-accelerator complex available for adsorption and maintains its level at an equilibrium value given by Eq. 6 and 7 that is quite low. That is why the current/voltage curves recorded in baths aged with a phosphorized copper anode rapidly stabilize with bath aging and why, for low accelerator concentrations, they appear at a more negative potential than those recorded when the bath is aged with a pure copper anode. This limitation of the amount of Cu^I complex explains why the inductive loop disappears during bath aging, except when this complex is stabilized by a large amount of accelerator (100 μM).

This theory can also explain why:

1. An increase in the MPSA concentration from 10 to 20 μM induces a shift of the current/voltage curves to less negative potentials whatever the aging anode material.

2. The hysteresis behavior disappears when a bath containing 20 μM of MPSA is aged: the amount of Cu^+ released in the bath as aging proceeds increases the bulk concentration of the Cu^I-accelerator complex and thus its surface coverage. The hysteresis can be attributed to a difference in the amount of additives adsorbed between the forward and the backward scan. If the Cu^I-accelerator complex surface coverage is increased, the inhibitor surface coverage is not favored and the forward scan proceeds at less negative potential as seen in Fig. 6a. Thus, when hysteresis behavior disappears, there is less differences in the complex surface coverage between forward and backward scan. Indeed, in this case, the disappearance of the hysteresis cannot be ascribed to the accelerator degradation, since copper deposition is highly accelerated and a large inductive loop (characteristic of the Cu^I-accelerator complex) is still present in the impedance spectra.

However, when the MPSA concentration is further increased in the plating bath up to 100 μM, the accelerating effect of MPSA is much lower than the one observed for a bath containing 20 μM MPSA. For comparison, Suarez and Olson[19] have shown with thiourea that, above a critical concentration between 26 and 79 μM, the thiourea inhibits copper deposition while, below this concentration, copper deposition is accelerated. They have also reported such behavior for other thiol compounds. Moreover, Dow et al.[8] have shown that, in the presence of both accelerator and chloride, the rate of copper deposition and the bath's superfilling ability depends on their respective concentration ratio. They also reported that the coordinating ability of thiolate is stronger than that of chloride ion and explain that if the thiolate/chloride concentration ratio is too high, Cu^I-accelerator complex directly bridges to the free copper surface and act as an inhibiting additive while, for lower ratios, the Cu^I-accelerator complex bridges to adsorbed chloride and then acts as an accelerating additive.

Thus, the anode material effect, the most striking effect observed in this study, can be easily explained by the fact that the phosphorus contained in the anode inhibits the Cu^+ release in the bath during anodic dissolution and therefore limits the formation of Cu^I-accelerator complex in the bulk to a value defined by Eq. 6 and 7.

The differences observed during aging between SPS-containing and MPSA-containing baths are consistent with the results of Dow et al.[8] that showed different behavior for these two additives that can only be explained if Reaction 2 is considered to be incomplete or negligible in the operating conditions used in this work. Such a difference is also observed in the case of thiourea, which is a thiol compound like MPSA, and its dimer (the FDS) which is a disulfide compound like SPS, that form two different complexes with cuprous ions.[19] In addition, our results obtained from the simulation of the impedance spectra obtained in fresh solutions of MPSA and SPS with various concentrations also suggest the formation of two different complexes between cuprous ions on one hand and MPSA or SPS on the other hand.[26] As a consequence, the Cu^I-accelerator complexes are most likely different in SPS or in MPSA-containing solutions. Because Frank and Bard[16] have shown that the Cu^I-accelerator ratios in the complex were, respectively, 1:1 and 1:2 for SPS and MPSA, Cu^ISPS should be formed in SPS-containing baths while $Cu^I(MPSA)_2$ is most probably formed in MPSA-containing solutions. In both cases, the Cu^I-accelerator bond involves ligand bonding between a lone pair of electrons of a sulfur atom and the 3d orbital of a copper ion.[2,8]

In addition, if the degradation is considered easier for MPSA (or $Cu^I(MPSA)_2$ complex) than for SPS (or Cu^ISPS complex), the apparent differences observed between the evolutions of the impedance spectra recorded during aging of MPSA and SPS containing baths with a pure copper anode can be explained. As far as a phosphorized copper anode is concerned, the small amount of Cu^+ released in the bath limits the amount of Cu^I-accelerator complex for whatever the accelerator molecule, and thus the inductive loop formation is limited (Fig. 9b and d).

However, to take into account the current density effect and the initial formation of an inductive loop in MPSA-containing baths aged with a phosphorized copper anode, some other phenomena must be occurring, as fresh baths do not exhibit such a loop.[26]

Whatever the anode material, copper dissolution is associated with the formation of a film at the electrode surface that contains different Cu^I products. For pure copper anodes, dissolution during long charging periods induces a large release of Cu^+ in the bath because the formed film (mainly CuCl) adheres poorly at the electrode surface.[20] This is not the case for a phosphorized copper because phosphorus entraps the electrogenerated Cu^+ in a stable black anodic film.[20] However, the formation of the black anodic film is not instantaneous. That is why copper interconnect electrodeposition manufacturers use a conditioning period to obtain a sufficiently thick black film before processing wafers so as to insure actual superfilling. As shown by Frankel et al.,[20] the film weight (and thus its thickness, if the film is considered as homogeneous) is directly proportional to the charge density (C/cm^2), and the curves obtained for different aging current density are very close to each other. As a consequence, this means that the growth rate of the black film is directly proportional to the anodic current density. Moreover, Rashov and Vuchkov[13] have shown that a sufficient overvoltage (i.e., a sufficiently high current density) is needed to initiate the black anodic film growth. This may explain why there are no significant differences between both anodic materials when aging proceeds at low anodic current density, i.e., at low growth rate of the film. Furthermore, if it is supposed that a very thin film does not prevent the Cu^+ release in the bath, it can be deduced that, in the very beginning of aging, a higher amount of Cu^I-accelerator com-

plex is formed as compared with a fresh bath. This explains why the impedance spectra recorded in baths aged at 25 mA/cm^2 exhibit an inductive loop that disappears when the bath ages (Fig. 9b). This behavior is not observed when the bath is aged at a 50 mA/cm^2 aging anodic current density, as shown by the initial values of D_{IL} in Fig. 11. Indeed, the film grows faster and Cu^+ release is more quickly inhibited. Because an increase in MPSA concentration from 10 to 20 μM stabilizes the Cu^I-accelerator complex, it can also explain why there is a higher initial amount of complex and why it takes longer to disappear as aging proceeds.

At this point, it is still necessary to explain why the influence of the bath aging is retarded when the anodic current density is increased, as clearly observed in Fig. 11. Healy et al.[14] have shown that either SPS or MPSA degrade by oxidation at the anode and that, when a Cu^I-accelerator complex is formed, it degrades at lower anodic potentials. In addition, the accelerator concentrations in the bath are very low (on the order of 10 μM) and thus it can be reasonably assumed that these reactions are mass transfer limited. As a consequence, the higher the anodic current density, the lower the ratio between the accelerator oxidation limiting current density and the applied current density. Therefore, for a given amount of charge passed in the bath, the degradation rate will be lower. Moreover, the higher the complex concentration in the bath, the higher its oxidation limiting current density and the faster it is degraded.

In addition, an odd but reproducible reduction wave was observed in CVs at the very beginning of the aging of the MPSA-containing baths, but only when they were aged with a phosphorized copper anode. The limiting current density is in the order of 3 $mA\ cm^{-2}$ and is associated with a product present at very low concentrations at the copper surface. Presently, we have not been able to clearly identify this reaction but find it interesting to report.

Conclusion

The addition of phosphorus in soluble copper anodes has a prominent effect on the evolution of copper plating behavior with bath aging, and its effect is more pronounced when the aging anodic current density is sufficiently high and when the accelerator concentration remains below or equal to 20 μM. The addition of phosphorus is characterized by a rapid stabilization of the current/voltage curves and of the impedance spectra during aging. Conversely, when a bath is aged with a pure copper anode, the copper deposition reaction is accelerated as compared with a bath aged with a phosphorized copper anode. The impedance spectra also exhibit an additional inductive loop whose size changes as aging proceeds.

These evolutions can be explained by the formation of a Cu^I-accelerator complex in the bulk of the bath and by the evolution of its concentration during aging. Indeed, this complex would require both Cu^+ and accelerator molecules for formation. Because the phosphorus inhibits the release of the Cu^+ ions in the plating bath by entrapment in the black anodic film, phosphorus inhibits complex formation, except when it is stabilized by a high accelerator concentration. The evolutions of current/voltage curves can be easily explained if the complex is considered as the species that adsorbs at the copper surface and that acts as the accelerator. In addition, the differences observed during aging between bath containing SPS and MPSA were explained by the different Cu^I-accelerator complexes formed in the SPS- or in the MPSA-containing solutions.

When the accelerator concentration is high (100 μM), its accelerating effect is lowered. This is consistent with the behavior reported in the literature for other thiol compounds which are known to act as inhibitors for concentrations in the order of the mmol/L.

The evolutions observed between both anode materials operating at very low current density were very similar and showed faster bath degradation. This was explained by the very slow increase of the black anodic film on the phosphorized copper anode which prevents the Cu^+ release into the solution and by an MPSA anodic degradation reaction that is mass transfer limited.

Centre National de la Recherche Scientifique assisted in meeting the publication costs of this article.

References

1. T. P. Moffat, D. Wheeler, W. H. Huber, and D. Josell, *Electrochem. Solid-State Lett.*, **4**, C26 (2001).
2. L. T. Koh, G. Z. You, S. Y. Lim, C. Y. Lim, and P. D. Foo, *Microelectron. J.*, **32**, 973 (2001).
3. T. P. Moffat, J. E. Bonevich, W. H. Huber, A. Stanishevsky, D. R. Kelly, G. R. Stafford, and D. Josell, *J. Electrochem. Soc.*, **147**, 4524 (2000).
4. K. R. Hebert, *J. Electrochem. Soc.*, **148**, C726 (2001).
5. N. Y. Kovarsky, Z.-W. Sun, and G. Dixit, in *Conference Proceedings ULSI XVII* (2002).
6. T. P. Moffat, D. Wheeler, and D. Josell, *J. Electrochem. Soc.*, **151**, C262 (2004).
7. W.-C. Tsai, C.-C. Wan, and Y.-Y. Wang, *J. Electrochem. Soc.*, **150**, C267 (2003).
8. W.-P Dow, H.-S. Huang, M.-Y. Yen, and H.-H. Chen, *J. Electrochem. Soc.*, **152**, C77 (2005).
9. E. Mattson and J. O'M. Bockris, *Trans. Faraday Soc.*, **55**, 1586 (1959).
10. J. O'M. Bockris and M. Enyo, *Trans. Faraday Soc.*, **58**, 1187 (1962).
11. O. R. Brown and H. R. Thirsk, *Electrochim. Acta*, **10**, 383 (1965).
12. F. Chao and M. Costa, *Bull. Soc. Chim. Fr.*, **10**, 4015 (1968).
13. S. Rashkov and L. Vuchkov, *Surf. Technol.*, **14**, 309 (1981).
14. J. P. Healy, D. Pletcher, and M. Goodenough, *J. Electroanal. Chem.*, **338**, 167 (1992).
15. J. P. Healy, D. Pletcher, and M. Goodenough, *J. Electroanal. Chem.*, **338**, 179 (1992).
16. A. Frank and A. J. Bard, *J. Electrochem. Soc.*, **150**, C244 (2003).
17. T. P. Moffat, B. Baker, D. Wheeler, and J. D. Josell, *Electrochem. Solid-State Lett.*, **6**, C59 (2003).
18. R. Palmans, S. Claes, L. E. Vanatta, and D. E. Colemand, *J. Chromatogr. A* **1085**, 147 (2005).
19. D. F. Suarez and F. A. Olson, *J. Appl. Electrochem.*, **22**, 1002 (1992).
20. G. S. Frankel, A. G. Schott, H. S. Isaacs, J. Horkans, and P. C. Andricacos, *J. Electrochem. Soc.*, **140**, 959 (1993).
21. L. Mirkova and S. Rashkov, *J. Appl. Electrochem.*, **24**, 420 (1994).
22. S. Goldbach, W. Messing, T. Daenen, and F. Lapicque, *Electrochim. Acta*, **44**, 323 (1998).
23. J. P. Healy, D. Pletcher, and M. Goodenough, *J. Electroanal. Chem. Interfacial Electrochem.*, **155**, 165 (1992).
24. M. L. Walker, L. J. Richter, and T. P. Moffat, *J. Electrochem. Soc.*, **152**, C403 (2005).
25. D. M. Soares, S. Wasle, K. G. Weil, and K. Doblhofer, *J. Electroanal. Chem.*, **532**, 353 (2002).
26. C. Gabrielli, P. Moçotéguy, H. Perrot, A. Zdunek, and D. Nieto-Sanz, *Electrochim. Acta*, **51**, 1462 (2006).
27. C. Gabrielli, P. Moçotéguy, H. Perrot, A. Zdunek, and D. Nieto-Sanz, and M. C. Clech, in *Copper Interconnects, Low-k Inter-level Dielectrics, and New Contact Metallurgies/Structures*, G. S. Mathad, H. S. Rathore, C. Reidsema-Simpson, K. Kondo, and V. Bakshi, Editors, PV 2003-10, p. 112, The Electrochemical Society Proceedings Series, Pennington, NJ (2003).
28. C. Gabrielli, P. Moçotéguy, H. Perrot, and R. Wiart, *J. Electroanal. Chem.*, **572**, 367 (2004).
29. C. Gabrielli, P. Moçotéguy, H. Perrot, A. Zdunek, and D. Nieto-Sanz, *J. Electrochem. Soc.*, Submitted.